

Nanofluid Flow Between Parallel Disks with Nernst-Planck Model

Shabnam ^a, Rehan Ali Shah ^a, Muhammad Sohail Khan ^a, Aamir Khan^{b*}

shabnam8688@gmail.com, mmrehan79@yahoo.com, sohaikhhan8688@gmail.com, aamir.khan@uoh.edu.pk

^a Department of Basic Sciences and Islamiat, University of Engineering and Technology Peshawar, KPK, Pakistan.

^bDepartment of Mathematics and Statistics, University of Haripur, 22620, KPK, Pakistan.

1 Abstract

This article explores a theoretical model that has been developed to analyze the behavior of a squeezing flow of nano-fluid between two disks. It has been further investigated that the uniform magnetic field is applied normal to the disks and an induced magnetic field is ignored due to the low Reynolds number. The domain of this study is to investigate the behavior of ionized flow in the radial and azimuthal direction with the change of non-dimensional parameters developed during modeling. The proposed theoretical model has been solved by a robust numerical scheme (PCM) and for the accuracy of this numerical scheme, the results have been compared with BVP4C.

Keywords: Nanoparticles, Lorentz force, Squeezing flow, Ionic distribution, Electric potential, PCM.

2 Introduction

There are many key applications of squeezing flow in science and technologies. These include the oil industry, hydrodynamic lubrication, biomechanics, polymer innovations, and aerodynamic heating. Due to its practical use in the food industry and chemical technology, research on the squeezing flow has been published in several journals over a century or more. The fundamental study in this area was done by Stefan [1] and he was the first one to adopt the method of lubrication and started distinguish work in the squeezing flow. In his investigation, he suggested the ad-hoc asymptotic approach for the solution of a Newtonian fluid. The analysis of the squeezing isothermal compressible film has been done by Salbu [2] in the absence of inertial effects. Thorp in [3] got the solution by taking the inertial effect. Kuzma [4] evaluated the behaviour of squeezing films between two circular

*Corresponding Author: aamir.khan@uoh.edu.pk

plates in the presence of inertial terms. However, later on, Gupta [5] demonstrated that this solution does not fulfil the given boundary conditions and is limited to a small value of Reynolds numbers. The current permissible study about all values of the Reynolds numbers in the lubrication problems has been done by Verma and Singh [6,7]. Siddiqui et al., [8] have used the hypothesis that the magnetic field employed orthogonally to the fluid flow between two endless surfaces and transformed the complicated form of Navier-stokes equations into a fourth-order ODEs. The flow is symmetrical and fulfills no-slip condition at $y=0$ at the upper layer and its estimated outcomes up to first order can be obtained. Ali et al. [9] investigated the oscillating behaviour of second-grade incompressible fluid flowing between porous half-space and the Laplace transform technique has been used to slowly evolve the solution of cosine and sine. Gupta and Rajagopal in [10] proposed an analytical solution for the second-grade fluid between two parallel plates through energy equation and the stability in the aforementioned flow is observed on the fixed amplitude disruptions. Hayat et al. [11] studied the influence of second-grade fluid through Laplace transform. Sheikholeslami et al. [12] have taken four different types of nanoparticles and investigated the behaviour of transient nanofluid flow through squeezing boundaries. It has been observed that the Nussult number and skin friction give higher values to silver than other nanoparticles. In addition, the Nussult number reveals robust dependency on the volumetric concentration of the nanoparticles. Timofeeva et al. [13] compared using different forms of nanoparticles to study their effects on thermal conductivity and concluded that blade-shaped nanoparticles give higher thermal conductivity. Hussain et al. [14] observed micro rotation impact on the flow of nanofluids and concluded that the existence of micro-rotation reduces the influence of skin friction coefficient and increases the heat transfer coefficient. It has been observed that the rate of heat transfer in Cu, Ag-water is less when compared to Cu, Ag-kerosene oil for different sizes of nanoparticles. Metal nanoparticles possess spherical shapes such as Cu, Ag and the nanotubes are having tube-shaped which may be single or multiple carbon nanotubes.

Heating/cooling is an essential work of trim and expulsion processes. One feature that has taken the heat transfer phenomenon to a whole new level is the inclusion of nanoparticles in the base fluid. It is a well-known fact that metals have a higher heat transfer capacity than commonly used liquids. As a result, the heat transfer of a base fluid containing metal particles is greater than that of normal base fluid. In addition, the size of the metal plays an important role, as big particles can come down under the influence of gravity due to the weight of the larger particles. The change which occurs due to the incorporation of ultrasmall size particles in the thermal conductivity of the base fluid is shown by Masuda et al. [15]. Hatami et al. [16] They investigated the flow of water-based nano-fluids in two contracting and rotating discs. The outcomes of this investigation show that by increasing the

injection, the temperature field becomes flattered near the centre of the channel, but in the case of expansion, the reverse trend is shown. In the above investigation, water-based nano-floats have been considered.

Industries such as manufacturing use a variety of fluids in many applications because of their high heat transfer capacity. Traditional liquids such as glycol, water, ethylene and kerosene are less capable of heat transfer. Choi in [17], for the first time, introduced the concepts of nanofluids and have taken their size (10-9 nm) and immersed them in the conventional base fluid. These nano-floats have high heat transfer capabilities and are especially useful in industrial applications. Nanofluids have four possible mechanisms that assist in heat transfer. they are: (a) clustering of nanoparticles in nanofluids, (b) ballistic type of thermal conduction in nanoparticles, (c) the liquid layer at the particle interface/ liquid and (d) Browning motion of nanoparticle. The browning motion of nanoparticles is very slow to transfer heat directly by nanofluid, still, it may have a fundamental role to induce convection such as particle clustering and a micro-environment around nanoparticles to enhance the heat transfer[18].Hughes et al. [19] were counted as the earliest researcher, who analyzed a straightforward elliptic and parabolic (MHD) flow in the magnetic field through computational fluid dynamics (CFD). Duwairi et al. [20] studied the properties of unidirectional squeezing flow and heat conduction of a viscid fluid in two parallel discs.

Probstein et al. [21], analyzed that the electroosmotic current is triggered by the electric field through the electric double layer and by the separation between the negative and positive ions formed by the capillary charged surface. In these systems and devices, the desired chemical species are supplied by instigating electroosmotic flow. When the liquid and channel walls are in contact with each other in a channel comprising an ionic liquid develop electrokinetic phenomena. In a liquid, the counter ions are drawn to the charged wall and form a protruding electric double layer which reduces the concentration of the counter ions from the wall. The diameter of the EDL may change from nanometer to micrometres, depends on the electrical characteristic of the fluid and ionic concentration, are analyzed by Lee et al. [22]. It has been analyzed by Davidson et al. [23] that the interface is affecting due to high-frequency error in the RDF plan as a result of taking high estimates. This technique was developed for wave break scene multimedia and scale interface. Park et al. [24] studied the behaviour of electroosmotic power and electrically fluid flow by formulating of Poisson-Boltzman equation. The fluid flow does not affect the ionic distribution. However, it has been acceptable to electroosmotic fluid flow in the microchannel, and there are many problems that have an unusual effect on the temperature of physical ions. The Poisson Boltzmann equation was compared to the Nernst Planck equation of electroosmotic liquid flow through channels, where the ideal ion involvement

is not specified. The nanofluids behaviour for flow and heat conduction between two parallel discs have been analyzed by Rizwan et al. [25]. We have taken suction/injection and the MHD on the bottom surface of the squeezing disk to observe the outcomes of two unlike nanofluids such as such as Cu-ethylene glycol and Cu-water. To investigate the flow and heat transfer behaviour on the surface, we have computed the numerical values of the skin friction coefficient and local Nusselt number. The result is based on a whole analysis that separates the flow and heat transfer properties of each mixture.

In the current article, we analyze the joint influence of the electromagnetic force, inertia force, surface suction or injection, magnetic field and ionized fluid in the squeezing flow of nanofluids between two parallel discs. In the squeezing flow, the aforementioned combination effect has not been studied before. The upper disk distributes negative ions uniformly while the lower one distributes positive ions. Further, the lower disk is permeable. Here, we want to study the behaviour of the fluid when the fluid becomes ionized. The numerical computation and graphical representation have been done for the Nussult number, velocity field, skin frictions, temperature and ions distribution respectively.

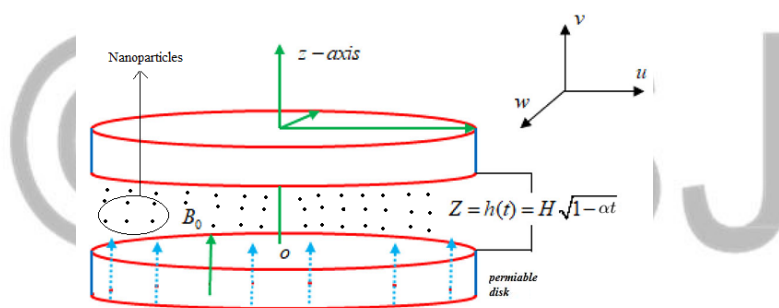


Figure 1: Geometry of the problem

3 Formulation

We consider a fully develop, incompressible,axisymmetric and transient flow of electroviscous fluid in the two parallel squeezing discs. The distance $h(t)$ is $H\sqrt{1-\alpha t}$ shows the separation between two discs and it is equal to l when $t = 0$ it is considered that the fluid comprise equilibrium cations (-) and anions (+) with values $z_+ = -z_- = z = 1$, spread evenly $a_+ = a_- = a$ and n_o is the bulk ion concentration of each species. Continuity and Navier-Stokes equation have been used to formulate the flow of electro-kinetic fluid with the electrical body. The Nernst Planck equation and Poisson-Boltzmann equation describes the stability of each ionic species and electrical potential of the charge distribution are incorporated in the aforementioned equations for fluid flow.

The mathematical formulation of the physical system are:

Continuity equation:

$$\frac{\partial u}{\partial r} + \frac{u}{r} + \frac{\partial w}{\partial z} = 0, \quad (1)$$

The Nondimensionalized Momentum equation in component form with electroviscous and magnetic effect:

$$\frac{\partial u}{\partial t} + u \frac{\partial u}{\partial r} + w \frac{\partial u}{\partial z} = -\frac{1}{\rho_{nf}} \frac{\partial P}{\partial r} + \frac{\mu_{nf}}{\rho_{nf}} \left(\frac{\partial^2 u}{\partial r^2} + \frac{1}{r} \frac{\partial u}{\partial r} - \frac{u}{r^2} + \frac{\partial^2 u}{\partial z^2} \right) + \frac{\sigma}{\rho_{nf}} B_0^2 u - BK^2 \nu_{nf}^2 (n^+ - n^-) \frac{\partial V}{\partial r} \quad (2)$$

$$\frac{\partial w}{\partial t} + u \frac{\partial w}{\partial r} + w \frac{\partial w}{\partial z} = -\frac{1}{\rho_{nf}} \frac{\partial P}{\partial z} + \frac{\mu_{nf}}{\rho_{nf}} \left(\frac{\partial^2 w}{\partial r^2} + \frac{1}{r} \frac{\partial w}{\partial r} + \frac{\partial^2 w}{\partial z^2} \right) - BK^2 \nu_{nf}^2 (n^+ - n^-) \frac{\partial V}{\partial z} \quad (3)$$

The Poisson equation:

$$\frac{\partial^2 V}{\partial r^2} + \frac{1}{r} \frac{\partial V}{\partial r} + \frac{\partial^2 V}{\partial z^2} = -\frac{1}{2} K^2 (n^+ - n^-) \quad (4)$$

The Nernst-Planck equations of Positive Ion:

$$\frac{\partial n^+}{\partial t} + u \frac{\partial n^+}{\partial r} + w \frac{\partial n^+}{\partial z} = \frac{\mu_{nf}}{Re S_c} \left(\frac{\partial^2 n^+}{\partial r^2} + \frac{1}{r} \frac{\partial n^+}{\partial r} + \frac{\partial^2 n^+}{\partial z^2} + \frac{\partial n^+}{\partial r} \frac{\partial V}{\partial r} + n^+ \frac{\partial^2 V}{\partial r^2} + \frac{\partial n^+}{\partial z} \frac{\partial V}{\partial z} + n^+ \frac{\partial^2 V}{\partial z^2} \right) \quad (5)$$

The Nernst-Planck equations of Negative Ion:

$$\frac{\partial n^-}{\partial t} + u \frac{\partial n^-}{\partial r} + w \frac{\partial n^-}{\partial z} = \frac{\mu_{nf}}{Re S_c} \left(\frac{\partial^2 n^-}{\partial r^2} + \frac{1}{r} \frac{\partial n^-}{\partial r} + \frac{\partial^2 n^-}{\partial z^2} - \frac{\partial n^-}{\partial r} \frac{\partial V}{\partial r} - n^- \frac{\partial^2 V}{\partial r^2} - \frac{\partial n^-}{\partial z} \frac{\partial V}{\partial z} - n^- \frac{\partial^2 V}{\partial z^2} \right) \quad (6)$$

The Equations of energy:

$$\frac{\partial T}{\partial t} + u \frac{\partial T}{\partial r} + w \frac{\partial T}{\partial z} = \frac{k_{nf}}{(\rho C_p)_{nf}} \left(\frac{\partial^2 T}{\partial r^2} + \frac{1}{r} \frac{\partial T}{\partial r} + \frac{\partial^2 T}{\partial z^2} \right) + \frac{\mu_{nf}}{(\rho C_p)_{nf}} \left(2 \left(\frac{\partial u}{\partial r} \right)^2 + \frac{\partial u}{\partial z} + 2 \frac{\partial u}{\partial z} \frac{\partial w}{\partial r} + \frac{2u^2}{r^2} + \left(\frac{\partial u}{\partial z} \right)^2 + 2 \left(\frac{\partial w}{\partial z} \right)^2 \right) \quad (7)$$

where C is the magnetic field, V is local total electrical potential induced, U is fluid velocity, $(\rho C_p)_{nf}$ is the heat capacity of the ionic nanofluid, p is fluid pressure, D is diffusion coefficient, T is the temperature, ρ_{nf} is fluid density of nanofluid, σ is electrical conductivity, S_c is Schmidt number, K^2 is the inverse Debye constant, κ_{nf} thermal conductivity of nanofluid, μ_{nf} is kinematic viscosity of nanofluid and the anions and cations are n^+ , n^- .

Nanofluid are defined as:

$$\nu_{nf} = \frac{\mu_{nf}}{\rho_{nf}}, \quad \rho_{nf} = \rho_f (1 - \phi + \phi \frac{\rho_s}{\rho_f}), \quad \mu_{nf} = \frac{1}{(1 - \phi)^{2.5}} \mu_f, \quad (8)$$

$$\kappa_{nf} = \kappa_f \frac{(\kappa_s + 2\kappa_f) - 2\phi(\kappa_f - \kappa_s)}{(\kappa_s + 2\kappa_f) + 2\phi(\kappa_f - \kappa_s)} \text{ and } (\rho C_p)_{nf} = (\rho C_p)_f (1 - \phi + \phi \frac{(\rho C_p)_s}{(\rho C_p)_f}),$$

with κ_f is the thermal conductivity of base fluid, κ_s is the thermal conductivity of the solid fraction and ϕ is the solid volume fraction of nanoparticles.

Boundary conditions

The boundary conditions are chosen as:

$$\begin{aligned}
 u = 0, \quad w = -\frac{dh}{dt}, \quad V = \frac{r^2}{2l(1-\alpha t)}, \quad n^- = 0, \quad n^+ = 0, \quad T = T_u \quad \text{at } z = h(t) \\
 u = 0, \quad w = -A, \quad V = 0, \quad T = 0, \quad n^+ = \frac{\alpha}{1-\alpha t}, \quad n^- = \frac{\alpha}{1-\alpha t}, \quad \text{at } z = 0
 \end{aligned} \tag{9}$$

The following similarity transformations are considered for the reducing PDE's (1 – 7) to ODE's system,

$$\begin{aligned}
 u = \frac{\alpha r}{2(1-\alpha t)} f'(\eta), \quad w = -\frac{\alpha H}{\sqrt{1-\alpha t}} f(\eta), \quad n^+ = \frac{\alpha \mu_f H(\eta)}{\rho_f (1-\alpha t)}, \quad n^- = \frac{\alpha \mu_f N(\eta)}{\rho_f (1-\alpha t)}, \\
 \theta(\eta) = \frac{T - T_h}{T_0 - T_h}, \quad V = \frac{r^2 Q(\eta)}{H^2(1-\beta t)}, \quad \text{where } \eta = \frac{z}{H\sqrt{1-\alpha t}}
 \end{aligned} \tag{10}$$

Therefore, equation (1) is satisfied and the remaining Eqs. (2 – 7) transform into the following form

$$\begin{aligned}
 f'''' = S(1-\phi)^{2.5}(1-\phi + \phi \frac{\rho_s}{\rho_f})(3f'' + \eta f'''' - 2ff''''') - (1-\phi)^{2.5} M f'' \\
 - \frac{2BK^2}{(1-\phi)^{2.5}(1-\phi + \phi \frac{\rho_s}{\rho_f})}(QH' + Q'H - Q'N - QN'),
 \end{aligned} \tag{11}$$

$$Q'' = -4Q - SK^2 K_1(H - N), \tag{12}$$

$$H'' = S_c S(1-\phi)^{2.5}(1-\phi + \phi \frac{\rho_s}{\rho_f})(\eta H' + 2H - 2H'f) - 2HQ - \delta Q'H' + \delta(4QH - SK^2 K_1(H^2 - HN)), \tag{13}$$

$$N'' = S_c S(1-\phi)^{2.5}(1-\phi + \phi \frac{\rho_s}{\rho_f})(\eta N' + 2N - 2N'f) + 2NQ + \delta Q'N' - \delta(4QN + SK^2 K_1(HN - N^2)), \tag{14}$$

$$\theta'' = SP_r \frac{(1-\phi + \phi \frac{(\rho C_p)_s}{(\rho C_p)_f})}{\frac{(\kappa_s + 2k_f) - 2\phi(\kappa_f - \kappa_s)}{(\kappa_s + 2k_f) + 2\phi(\kappa_f - \kappa_s)}} (\eta \theta' - \theta'f) - \frac{PrEc}{(1-\phi)^{2.5} \frac{(\kappa_s + 2k_f) - 2\phi(\kappa_f - \kappa_s)}{(\kappa_s + 2k_f) + 2\phi(\kappa_f - \kappa_s)}} (6f'^2 + \delta f''^2). \tag{15}$$

and the transform boundary conditions are

$$\begin{aligned}
 f(0) = A, \quad f'(0) = 0, \quad Q(0) = 0, \quad H(0) = 1, \quad N(0) = 1, \quad \theta(0) = 1, \\
 f(1) = \frac{1}{2}, \quad f'(1) = 0, \quad Q(1) = 1, \quad H(1) = 0, \quad N(1) = 0, \quad \theta(1) = 0,
 \end{aligned} \tag{16}$$

where $S_c = \frac{\mu}{\rho D}$ Schmidt number, $S = \frac{\alpha H^2}{2\nu}$ squeeze number, $Pr = \frac{\mu_f(\rho C_p)_f}{\kappa_f}$ Prandtl number, $Ec = \frac{1}{(C_p)_f(T_0 - T_u)} (\frac{\alpha H}{2(1-\alpha t)})^2$ Eckert number, $\delta = \frac{r^2}{H^2(1-\alpha t)}$, $B = \frac{\rho k^2 T^2 \epsilon_0 \epsilon}{2z^2 e^2 \mu^2}$ is fixed at a specified temperature, $K_1^2 = \frac{2z^2 e^2 H^2 n_0}{\epsilon_0 \epsilon k_b T}$ the dimensionless inverse of Debye length, $M = \frac{H^2 \sigma B_0^2 (1\alpha t)}{\rho_f \nu_f \mu_e}$ Hartman number, $\Omega = \frac{T_u}{T_l}$ and $\lambda = \frac{\nu}{\rho}$.

Required physical parameters are the Nusselt number and skin friction coefficient, which can be defined as,

$$C_f = \frac{\mu_{nf}}{\rho_{nf} (\frac{-\alpha l}{2\sqrt{1-\alpha t}})^2} (\frac{\partial u}{\partial z} + \frac{\partial u}{\partial r})_{z=h(t)}, \quad N_u = -\frac{\kappa_n f (\frac{\partial T}{\partial z})_{z=h(t)}}{k_f (T_0 - T_u)}, \tag{17}$$

In case of Eq.(16), we get

$$\frac{H^2(1-\phi)^{2.5}(1-\phi+\phi\frac{\rho_s}{\rho_f})}{r^2} ReC_f = f''(1), \quad -\theta'(0) = \frac{H\sqrt{1-\alpha t}}{\frac{\kappa_s+2\kappa_f-2\phi(\kappa_f-\kappa_s)}{\kappa_s+2\kappa_f+2\phi(\kappa_f-\kappa_s)}} Nu. \quad (18)$$

4 Analytic Solution by PCM

In this section, optimal choices of continuation parameters are made through the algorithm of PCM for the solution of non-linear equations (11 – 15) with boundary conditions in equation (16):

• First order of ODE

To transform the equations (11 – 15) into first order of ODE's, consider the following

$$\begin{aligned} f &= p_1, & f' &= p_2, & f'' &= p_3, & f''' &= p_4 \\ Q &= p_5, & Q' &= p_6, & H &= p_7, & H' &= p_8 \\ N &= p_9, & N' &= p_{10}, & \theta &= p_{11}, & \theta' &= p_{12} \end{aligned} \quad (19)$$

putting these transformations in Eqs. (11 – 15), which becomes

$$\begin{aligned} p'_4 &= S(1-\phi)^{2.5}(1-\phi+\phi\frac{\rho_s}{\rho_f})(3p_3+\eta p_4-2p_1p_4) - (1-\phi)^{2.5}Mp_3 \\ &\quad - \frac{2BK^2}{(1-\phi)^{2.5}(1-\phi+\phi\frac{\rho_s}{\rho_f})}(p_5p_8+p_6p_7-p_6p_9-p_5p_{10}), \end{aligned} \quad (20)$$

$$p'_6 = -4p_5 - SK^2K_1(p_7 - p_9), \quad (21)$$

$$\begin{aligned} p'_8 &= S_cS(1-\phi)^{2.5}(1-\phi+\phi\frac{\rho_s}{\rho_f})(\eta p_8+2p_7-2p_1p_8) - 2p_5p_7 - \delta p_8p_8 \\ &\quad + \delta(4p_5p_7 - SK^2K_1(p_7^2 - p_7p_9)), \end{aligned} \quad (22)$$

$$\begin{aligned} p'_{10} &= S_cS(1-\phi)^{2.5}(1-\phi+\phi\frac{\rho_s}{\rho_f})(\eta p_{10}+2p_9-2p_1p_{10}) + 2p_5p_9 + \delta p_6p_{10} \\ &\quad - \delta(4p_5p_9 + SK^2K_1(p_7p_9 - p_9^2)), \end{aligned} \quad (23)$$

$$\begin{aligned} p'_{12} &= SPr \frac{(1-\phi+\phi\frac{(\rho Cp)_s}{(\rho Cp)_f})}{\frac{(\kappa_s+2k_f)-2\phi(\kappa_f-\kappa_s)}{(\kappa_s+2k_f)+2\phi(\kappa_f-\kappa_s)}} (\eta p_{12} - p_1p_{12}) \\ &\quad - \frac{PrEc}{(1-\phi)^{2.5}\left(\frac{(\kappa_s+2k_f)-2\phi(\kappa_f-\kappa_s)}{(\kappa_s+2k_f)+2\phi(\kappa_f-\kappa_s)}\right)} (6p_2^2 + \delta p_3^2), \end{aligned} \quad (24)$$

and the boundary conditions becomes

$$\begin{aligned} p_2(0) &= 0, & p_1(0) &= A, & p_2(1) &= 0, & p_1(1) &= \frac{1}{2}, & p_5(0) &= 0, & p_5(1) &= 1, \\ p_7(0) &= 1, & p_7(1) &= 0, & p_9(0) &= 1, & p_9(1) &= 0, & p_{11}(0) &= 1, & p_{11}(1) &= 0, \end{aligned} \quad (25)$$

• **Introducing of parameter p and we obtained ODEs in a p-parameter group**

To get ODE's in a p-parameter group, let we know p-parameter in Eqs. (20 – 24) and therefore,

$$p'_4 = S(1 - \phi)^{2.5} (1 - \phi + \phi \frac{\rho_s}{\rho_f}) (3p_3 + \eta p_4 - 2p_1(p_4 - 1)q) - (1 - \phi)^{2.5} M p_3 - \frac{2BK^2}{(1 - \phi)^{2.5} (1 - \phi + \phi \frac{\rho_s}{\rho_f})} (p_5 p_8 + p_6 p_7 - p_6 p_9 - p_5 p_{10}), \tag{26}$$

$$p'_6 = -4p_5 - SK^2 K_1 (p_7 - p_9 + p_6 - (p_6 - 1)q), \tag{27}$$

$$p'_8 = S_c S (1 - \phi)^{2.5} (1 - \phi + \phi \frac{\rho_s}{\rho_f}) (\eta p_8 + 2p_7 - 2p_1(p_8 - 1)q) - 2p_5 p_7 - \delta p_8 p_8 + \delta (4p_5 p_7 - SK^2 K_1 (p_7^2 - p_7 p_9)), \tag{28}$$

$$p'_{10} = S_c S (1 - \phi)^{2.5} (1 - \phi + \phi \frac{\rho_s}{\rho_f}) (\eta p_{10} + 2p_9 - 2p_1(p_{10} - 1)q) + 2p_5 p_9 + \delta p_6 p_{10} - \delta (4p_5 p_9 + SK^2 K_1 (p_7 p_9 - p_9^2)), \tag{29}$$

$$p'_{12} = SP r \frac{(1 - \phi + \phi \frac{(\rho C p)_s}{(\rho C p)_f})}{\frac{(\kappa_s + 2k_f) - 2\phi(\kappa_f - \kappa_s)}{(\kappa_s + 2k_f) + 2\phi(\kappa_f - \kappa_s)}} (\eta p_{12} - p_1(p_{12} - 1)q) - \frac{PrEc}{(1 - \phi)^{2.5} \frac{(\kappa_s + 2k_f) - 2\phi(\kappa_f - \kappa_s)}{(\kappa_s + 2k_f) + 2\phi(\kappa_f - \kappa_s)}} (6p_2^2 + \delta p_3^2). \tag{30}$$

• **Differentiation by p, reaches at the following system w.r.t the sensitivities to the parameter-p**

Differentiating the Eqs. (26 – 30) w.r.t by p

$$d'_1 = h_1 d_1 + e_1 \tag{31}$$

where h_1 is the coefficient matrix, e_1 is the remainder and $d_1 = \frac{dp_i}{d\tau}$, $1 \leq i \leq 12$.

• **Cauchy Problem**

$$d_1 = y_1 + a_1 v, \tag{32}$$

where y_1, v are vector functions. By resolving the two Cauchy problems for every component.

We are satisfied then automatically to ODE's

$$e_1 + h_1(a_1 v + y_1) = (a_1 v + y_1)' \tag{33}$$

and left the boundary conditions.

• **Using by Numerical Solution**

An absolute scheme has been used for the resolution of the problem

$$\frac{v^{i+1} - v^i}{\Delta \eta} = h_1 v^{i+1} \tag{34}$$

$$\frac{y^{i+1} - y^i}{\Delta \eta} = h_1 y^{i+1} + e_1 \tag{35}$$

• **Taking of the corresponding coefficients**

As given boundaries are usually applied for p_i , where $1 \leq i \leq 12$, for the solution of ODE's, we required to apply $d_2 = 0$, which seems to be in matrix form as

$$l_1.d_1 = 0 \text{ or } l_1.(a_1v + y_1) = 0 \tag{36}$$

where $a_1 = \frac{-l_1.y_1}{l_1.v}$

Table 1: The thermophysical properties of water base fluid and Fe_3O_4 nanoparticles.

	ρ	C_p	κ	σ
H_2O	997.1	4179	0.613	5.5×10^{-6}
Fe_3O_4	5200	670	6	9.74×10^6

5 Results and Discussions

In order to analyze the flow and heat transfer behavior we have displayed the numerical results of radial velocity $f(\eta)$, velocity profile $f'(\eta)$, Poisson $Q(\eta)$, positive ion $H(\eta)$, negative ion $N(\eta)$ and temperature profile $\theta(\eta)$ for the different values of emerging parameters such as suction/injection parameter, squeeze number S , nanoparticle volume fraction and Hartman number M respectively. In the graphical representation the following domain $0 \leq \eta \leq 1$ for the variable η has been used. The numerical results obtained by two numerical schemes (BVP4C and PCM) are compared and displayed in table 2. The numerical results of Nusselt number and skin friction for different values of nanoparticle volume fraction ϕ are given in table 3.

The influence of squeezing parameter S over the horizontal velocity $f(\eta)$ of the nanofluid flow is shown in Figure 2(a). Particularly, it is worth noting that the negative value of the squeezing number refers to diminishing the flow channel. Increasing absolute values of $S < 0$ increases the horizontal velocity. The effect of squeezing number S over the vertical component of the velocity field is displayed in Figure 2(b). It is obvious from Figure 2(a) that the movement of the upper plate in the direction of the lower plate shoves the fluid in the vertical direction. An opposite force is producing to the vertical component due to a rise in the normal velocity ($S = -1.5, -4.5, -8.5$) of the upper disk toward the lower disk and hence, the fluid tends to flows in the horizontal direction. In the vicinity of the lower disk, the effect of vertical velocity is dominated by the normal velocity. Nevertheless, when the fluid passes through the center, the vertical velocity dominates the horizontal velocity as a result $f'(\eta)$ is decreasing. The ions distribution profile becoming stronger when it moves from the lower disk to the

upper one is explicitly shown in Figure 3(a-b). Figure 3(c) is made to display the influence of the squeezing parameter on Poisson distribution. The decrease in the potential energy in the centre of the fluid domain is plotted in Fig. 3(c).

The influence of M on $f'(\eta)$ and $f(\eta)$ is plotted in Figure 4(a-b). The horizontal velocity is getting increase due to the increase of M as shown in Fig 4(a). Hence, the magnetic parameter can be used to increase the horizontal velocity of the fluid. It is noticed that the rise in the value of M grows the vertical velocity within $\eta < 0.5$ for assisting cases, otherwise, its influence is reversed. Similarly, the effect of M in the domain where $\eta > 0.5$ works in the reverse direction of the fluid flow which decreases the velocity of the fluid is shown in Figure 4(b). Figure 4(a-b) displays the influence of the M on $f(\eta)$ and $f'(\eta)$. Figure 5(a-b) illustrate the effect of Ec and S on heat transfer. It has been noticed that with increasing the values of Ec and S , the behavior of fluid temperature increases continuously, as a resistive force that goes up the motion of particles. Hence, the heat transfer is produced and temperature increases. Temperature increases as a function of Ec due to an increase in the kinematic viscosity and diffusivity and the molecules become more mobile by increasing the values of Ec and S as shown in Fig 5(a-b). The influence of Sc on ions distributions $H(\eta)$ and $N(\eta)$ is displayed in Fig. 6(a). It shows that an increase in Schmidt number Sc decrease the cation distribution because of the size of the ionic radius decreases and the loss of electrons for $0 \leq \eta \leq 0.55$. It is true due to the electrically conducting fluid in the presence of uniform magnetic field, which slow down the fluid motion in the boundary layer region. But for $\eta > 0.56$ the reverse influence is increased. It is seen that the anions distribution gradually increases with Sc increases in Fig 6(b). The effect of K on poisson distribution is shown in Fig. 7(a). The increase in K decreases the electrical potential energy. Therefore, the poisson distribution decreases due to separations of electrons. The effect of K on cation distributions is displayed in Fig. 7(b). By increasing the vales of K , the distribution of cations from the lower disk to the upper disk is getting stronger due to the electric potential energy.

Table 2: Comparison of PCM numerical results with that of BVP4C, for the physical parameters, $S = -1.5, M = 0.5, B = 1.5, K = 0.5, K_1 = 0.9, Sc = 2.5, \delta = 1.5, Pr = 6.2$ and $Ec = 1.5$

η	PCM					BVP4C				
	$f''(\eta)$	$Q'(\eta)$	$H'(\eta)$	$N'(\eta)$	$\theta'(\eta)$	$f''(\eta)$	$Q'(\eta)$	$H'(\eta)$	$N'(\eta)$	$\theta'(\eta)$
0	4.3782	-1.2520	2.5048	-11.6047	-3.9273	4.3780	-1.2522	2.5042	-11.6050	-3.9270
0.1	4.2079	-1.2539	2.1728	-11.4206	-3.8250	4.2073	-1.2540	2.1726	-11.4200	-3.8253
0.2	4.0409	-1.2563	1.8475	-11.2472	-3.7250	4.0411	-1.2567	1.8470	-11.2476	-3.7251
0.3	3.8774	-1.2596	1.5317	-11.0840	-3.6274	3.8779	-1.2590	1.5318	-11.0844	-3.6270
0.4	3.7176	-1.2638	1.2283	-10.9294	-3.5324	3.7170	-1.2630	1.2289	-10.9298	-3.5322
0.5	3.5616	-1.2690	0.9407	-10.7786	-3.4400	3.5611	-1.2696	0.9400	-10.7782	-3.4401
0.6	3.4095	-1.2752	0.6722	-10.6223	-3.3504	3.4099	-1.2758	0.6727	-10.6228	-3.3510
0.7	3.2616	-1.2817	0.4264	-10.4417	-3.2633	3.2610	-1.2813	0.4260	-10.4414	-3.2637
0.8	3.1181	-1.2869	0.2077	-10.2045	-3.1788	3.1186	-1.2865	0.2071	-10.2040	-3.1790
0.9	2.9795	-1.2882	0.0210	-9.8621	-3.0966	2.9797	-1.2880	0.0218	-9.8624	-3.0961
1.0	2.8467	-1.2817	-0.1285	-9.3607	-3.0165	2.8460	-1.2812	-0.1288	-9.3601	-3.0170

Table 3: The numerical result of Skin friction and Nusselt number for water functionalized Cu nanoparticle with the different values of volume fraction ϕ and suction parameter $A = 1$. With various physical parameters values are $B = 1.5, K = 0.5, K_1 = 0.9, Sc = 2.5, \delta = 10, Pr = 6.2$ and $Ec = 0.5$

η	S = 0.5		M = 2	
	$f''(1)$	$-\theta'(0)$	$f''(1)$	$-\theta'(0)$
0	2.7519	7.3676	2.7215	7.3732
0.2	2.8293	7.2082	2.7996	7.2120
0.4	2.9082	7.0549	2.8793	7.0570
0.6	2.9886	6.9073	2.9604	6.9077
0.8	3.0704	6.7650	3.0430	6.7640
1.0	3.1537	6.6278	3.1272	6.6255

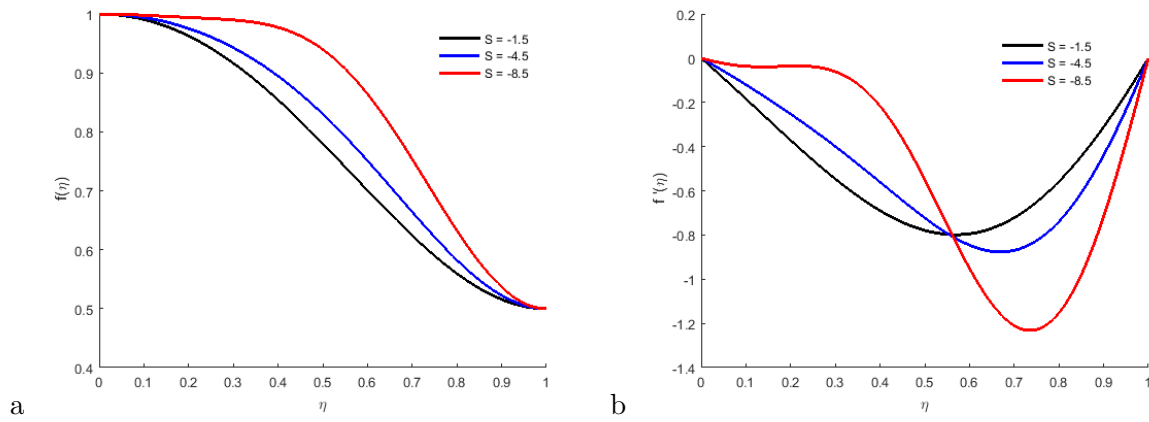


Figure 2: Influence of $f(\eta)$ and $f'(\eta)$ for S and fixed values of $M = 0.50, B = 1.5, K = 0.5, K_1 = 0.9, Sc = 2.5, \delta = 1.5, Pr = 6.2, Ec = 1.5$.

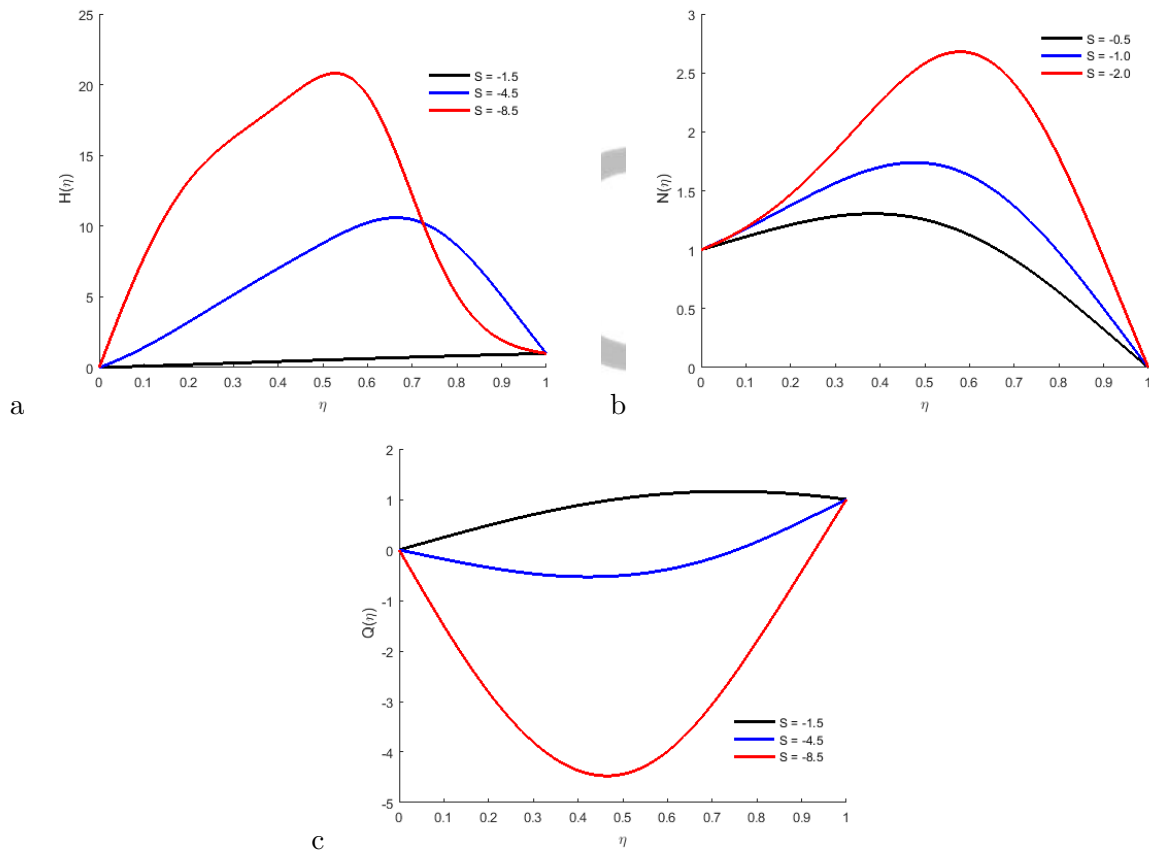


Figure 3: Influence of $H(\eta), N(\eta)$ and $Q(\eta)$ for S and fixed values of $M = 0.5, B = 1.5, K = 0.5, K_1 = 0.9, Sc = 2.5, \delta = 1.5, Pr = 6.2, Ec = 1.5$.

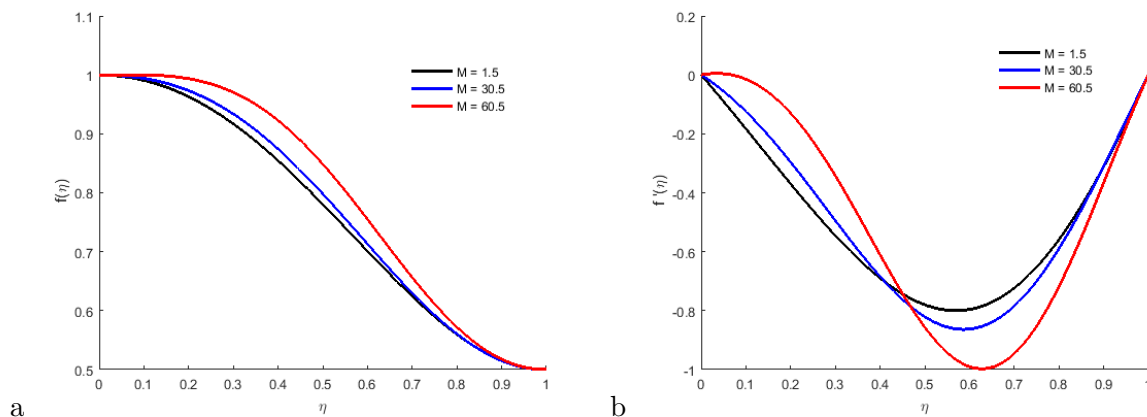


Figure 4: Influence of $f(\eta)$ and $f'(\eta)$ for M and fixed values of $S = -1.5, B = 1.5, K = 0.5, K_1 = 0.9, Sc = 2.5, \delta = 1.5, Pr = 6.2, Ec = 1.5$.

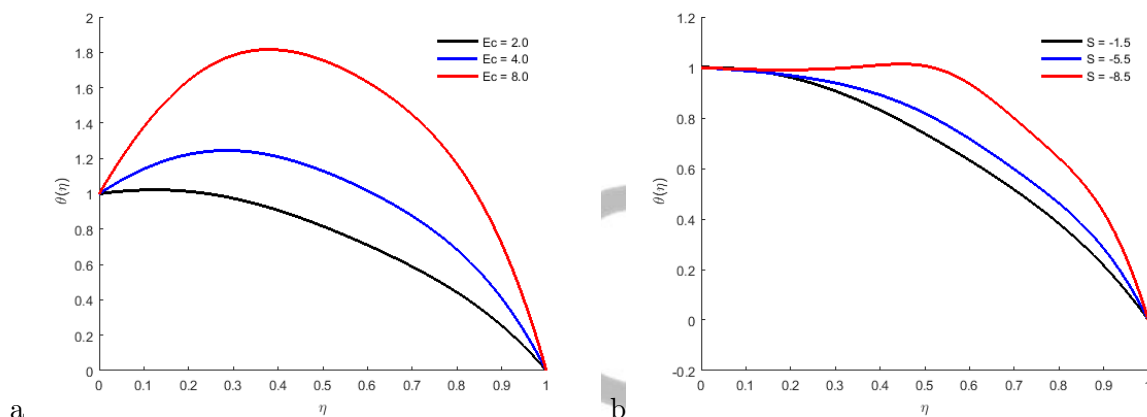


Figure 5: Influence of $\theta(\eta)$ for Pr, Ec, S and fixed values of $B = 1.5, K = 0.5, K_1 = 0.9, Pr = 6.2, M = 0.5, \delta = 1.5, Sc = 2.5$.

6 Concluding Remarks

In the current study, the similarity transformation solution is achieved for the modeled system of ODEs in (10 – 14). The Navier-Stokes equation, energy equation, Poisson and Nernst-Planck equations are coupled with the system of non-linear ODE's. The similarly equations have been solved by using PCM.

Following conclusions are drawn:

- The increase in the normal velocity of the upper disk towards the lower disk is producing the opposite force of the vertical component, and thus the fluid moves in a horizontal direction.
- The influence of the squeezing parameter on Poisson distributions shows that potential energy decreases in the centre of the fluid domain.

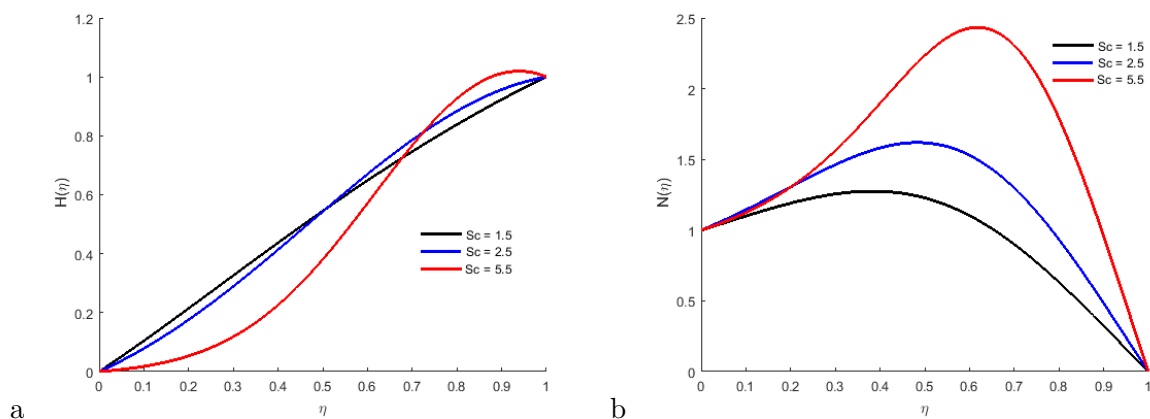


Figure 6: Influence of $H(\eta)$ and $N(\eta)$ for Sc and fixed values of $S = -1.5, B = 1.41, K = 0.2, K_1 = 0.5, M = 0.41, \delta = 1, Pr = 6.2, Ec = 0.5$.

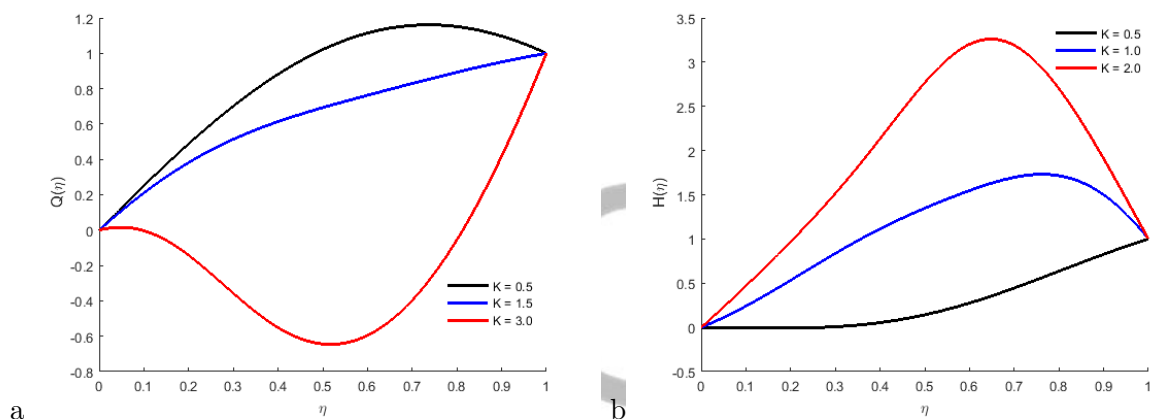


Figure 7: Influence of $Q(\eta)$ and $H(\eta)$ for K and fixed values of $S = -1.5, M = 0.5, B = 1.5, K_1 = 0.9, Sc = 2.5, \delta = 1.5, Pr = 6.2, Ec = 1.5$.

- It shows that an increase in Schmidt number Sc decreases the cation distribution because of the size of the ionic radius decreases and the loss of electrons in the region $0 \leq \eta \leq 0.55$.
- The influence of the squeezing parameter on the horizontal velocity $f(\eta)$ of the nano-fluid flow. Here, it is worth noting that the negative squeeze number refers to narrowing the flow channel.
- It is shown that as squeezing number increases the positive ions decreases due to the loss of electrons.

References

- [1] J. Stefan Versuche über die scheinbare Adhäsion, Sitzungsberichte der kaiserlichen Akademie der Wissenschaften. Mathematisch Naturwissenschaftliche Classe, Band II, Abteilung Wien. 69, (1874), 713-735.
- [2] E. O. Salbu, Compressible Squeeze Films and Squeeze Bearings. J Basic Eng., 86, (1964), 355.
- [3] J. F. Thorpe, W. A. Shaw, Developments in Theoretical and Applied Mechanics. Pergamon Press, Oxford, (1967).
- [4] D. C. Kuzma, Fluid Inertia Effects in Squeeze Films. Applied Scientific Research, 18, (1968), 15-20.
- [5] P. S. Gupta, A. S. Gupta, Squeezing Flow Between Parallel Plates. Wear, 45, (1977), 177-185.
- [6] R. L. Verma, A Numerical Solution for Squeezing Flow Between Parallel Channels, Wear. 72, (1981) 89-95.
- [7] P. Singh, Radhakrishnan V, Narayan K. A, Squeezing Flow Between Parallel Plates. Ingénieur-Archives, 60, (1990), 274-281.
- [8] Siddiqui A, Irum S and Ansari A. Unsteady squeezing flow of a viscous MHD fluid between parallel plates, a solution using the homotopy perturbation method. Math Model Anal 2008; 2: 565-576.
- [9] Ali F, Norzieha M, Sharidan M, et al. New exact solutions of Stokes-second problem for an MHD second grade fluid in a porous space. Int J Non Linear Mech 2012; 47: 521-525.
- [10] Gupta A and Rajagopal K. Flow and stability of a second grade fluid between two parallel plates rotating about noncoincident axes. Int J Eng Sci 1981; 19: 1401-1409.
- [11] Hayat T, Ellahi R, Asghar S, et al. Flow induced by non-coaxial rotation of a porous disk executing nontorsional oscillations and a second grade fluid rotating at infinity. Appl Math Modell 2004; 28: 591-605.
- [12] M. Sheikholeslami , D.D. Ganji , H.R. Ashorynejad, Investigation of squeezing unsteady nanofluid flow using ADM, Powder Technology, 239 (2013), 259-265.
- [13] E. V. Timofeeva, J. L. Routbort, D. Singh, Particle shape effects on thermophysical properties of alumina nanofluids, Journal of Applied Physics, 106 (1) (2009), 014304.

- [14] S.T. Hussain, S. Nadeem, R. U. Haq, Model-based analysis of micropolar nanofluid flow over a stretching surface, *European Physical Journal Plus*, 129 (2014), 161.
- [15] H. Masuda, A. Ebata, K. Teramae, N. Hishinuma, Alteration of Thermal Conductivity and Viscosity of Liquid by Dispersing Ultra-Fine Particles, *Netsu Bussei* ,7(4) (1993), 227-233.
- [16] M. Hatami, M. Sheikholeslami, D.D. Ganji, Laminar flow and heat transfer of nanofluid between contracting and rotating disks by least square method, *Powder Technology*, 253 (2014), 769-779.
- [17] Choi SUS, Eastman JA Enhancing thermal conductivity of fluids with nanoparticles. Proceedings of the 1995 ASME International Mechanical Engineering Congress and Exposition, San Francisco, USA, ASME FED 231/ MD 66:99,105, 1995.
- [18] M. Azimi, F. Ommi Using nanofluid for heat transfer enhancement in engine cooling process *Nano Energy and Power Research*, 2 (2013), pp. 1-3
- [19] M. Hughes, K.A. Pericleous, M. Cross. The CFD analysis of simple parabolic and elliptic MHD flows *Applied Mathematics Modeling*, 18 (1994), pp. 150-155.
- [20] Duwairi, H.M., Tashtoush, B., Domeshe, R.A.: On heat transfer effects of a viscous fluid squeezed and extruded between parallel plates. *Heat Mass Transfer* 14, 112-117 (2004).
- [21] R.F. Probst, *Physicochemical Hydrodynamics*, Wiley, New York, 1994.
- [22] C.-Y. Lee, G.-B. Lee, J.-L. Lin, F.-C. Huang, C.-S. Liao, *J. Micromech. Microeng.* 15 (2005) 1215-1223.
- [23] M. R. Davidson, D. J. E. Harvie, Electroviscous effects in low Reynolds number liquid flow through a slit-like microfluidic contraction, *Chem. Eng. Sci.*, 62, (2007) 4229-4240.
- [24] H. M. Park, J. S. Lee, T. W. Kim, Comparison of the Nernst-Planck model and the Poisson-Boltzmann model for electroosmotic flows in microchannels, *Journal of Colloid and Interface Science*, 315, (2007) 731-739.
- [25] Rizwan H., Khan Z. H., Hussain S. H., "Flow and heat transfer analysis of Water and Ethylene glycol based Cu nanoparticles between two parallel disks with suction/injection effects". *The Journal of Molecular Liquids*. 221, 298-304, (2016).